

UC Irvine

UC Irvine Previously Published Works

Title

Historical spatiotemporal changes in fire danger potential across biomes

Permalink

<https://escholarship.org/uc/item/7ph093nx>

Authors

Baijnath-Rodino, Janine A

Le, Phong VV

Foufoula-Georgiou, Efi

et al.

Publication Date

2023-04-01

DOI

10.1016/j.scitotenv.2023.161954

Copyright Information

This work is made available under the terms of a Creative Commons Attribution License, available at <https://creativecommons.org/licenses/by/4.0/>

Peer reviewed



Historical spatiotemporal changes in fire danger potential across biomes

Janine A. Bajjnath-Rodino ^{a,*}, Phong V.V. Le ^{a,b,c}, Efi Foufoula-Georgiou ^{a,d}, Tirtha Banerjee ^a

^a Department of Civil and Environmental Engineering, University of California-Irvine, Irvine, CA, USA

^b Faculty of Hydrology Meteorology and Oceanography, University of Science, Vietnam National University, Hanoi, Viet Nam

^c Environmental Sciences Division, Oak Ridge National Laboratory, Oak Ridge, TN, USA

^d Department of Earth Systems Science, University of California-Irvine, Irvine, CA, USA



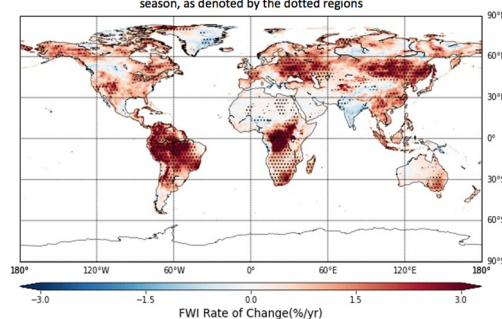
HIGHLIGHTS

- Quantifying spatial and seasonal changes in fire danger potential and fire behavior potential across different ecosystems
- SON exhibits the greatest rate of increase in fire danger potential, followed by JJA, DJF, and MAM.
- The temperate biomes exhibit the greatest rate of increases in fire danger potential and fire behavior potential.
- The Mangrove Biome exhibits the least increase in fire danger potential and fire behavior potential.

GRAPHICAL ABSTRACT

Within the past four decades, the number of wildfires and wildfire size have been increasing in many regions of the world. However, understanding the seasonal and ecoregion changes in fire danger potential and fire behavior potential as they relate to changes in fire weather conditions, remain under-explored. Therefore, this study 1) identifies the seasons and biomes that exhibit significant (1980–2019) changes in fire danger potential; 2) explores what types of fire behavior potentials may be influencing changes in fire danger potential; 3) determine how fire danger potential and fire behavior potential follow similar responses to that of changes in seasonal mean temperature and seasonal precipitation totals. Fire danger potential is determined by using the Canadian Fire Weather Index. Fire behavior potential is determined by the US Energy Release Component, and Ignition Component. Results indicate that the Boreal Fall has been experiencing the greatest increase in fire danger potential, followed by the Boreal Summer, Winter, and Spring. The increase in fire danger potential is predominant over the Tropical and Subtropical Moist Broadleaf Forest Biome, as well as all vegetation types of the temperate biomes. Similarly, the temperate biomes experience the greatest rate of increase in fire intensity potential and ignition potential, but this is prevalent during the Boreal Winter and Spring. There is also a positive and significant correlation between fire danger potential and seasonal mean air temperature during the Boreal Summer in the Northern Hemisphere for the temperate biomes in North America and Europe, as well as the Tropical and Subtropical biomes in Africa. Our study shows how fire danger potential and fire behavior potential have been responding to changes in seasonal mean temperature and seasonal precipitation totals across different ecoregions around the world.

The 1980–2019 significant rate of change in fire danger potential (%/yr) for the SON season, as denoted by the dotted regions



ARTICLE INFO

Editor: Manuel Esteban Lucas-Borja

Keywords:
Wildfires
Biomes

ABSTRACT

This study 1) identifies the seasons and biomes that exhibit significant (1980–2019) changes in fire danger potential, as quantified by the Canadian Fire Weather Index (FWI); 2) explores what types of fire behavior potentials may be contributing to changes in fire danger potential, as quantified by the United States Energy Release Component (ERC) and the Ignition Component (IC); 3) provides spatiotemporal insight on how fire danger potential and fire behavior potential are responding in relation to changes in seasonal precipitation totals and seasonal mean air temperature across

* Corresponding author.

E-mail address: jbajjnath@uci.edu (J.A. Bajjnath-Rodino).

<http://dx.doi.org/10.1016/j.scitotenv.2023.161954>

Received 17 May 2022; Received in revised form 27 January 2023; Accepted 28 January 2023

Available online 2 February 2023

0048-9697/© 2023 The Authors. Published by Elsevier B.V. This is an open access article under the CC BY license (<http://creativecommons.org/licenses/by/4.0/>).

Fire danger potential
 Fire intensity
 Ignition component
 Drought

biomes. Time series of these fire potentials, as well as seasonal mean temperature, and seasonal precipitation totals are generated using data from the 0.25° ECMWF spatial resolution Reanalysis 5th Generation (ERA5) and the Climatic Research Unit gridded Time Series (CRU TS). The Mann-Kendall test is then applied to identify significant spatiotemporal trends across each biome. Results indicate that the September–November season (SON) exhibits the greatest rate of increase in fire danger potential, followed by the June–August season (JJA), December, January–February season (DJF), and March–May season (MAM), and this is predominant over the Tropical and Subtropical Moist Broadleaf Forest Biome, as well as all vegetation types of the temperate biomes. Similarly, the temperate biomes experience the greatest rate of increase in fire intensity potential and ignition potential, but prevalent during the DJF and MAM seasons. Furthermore, there is a significant positive correlation between fire danger potential and seasonal mean air temperature during JJA in the Northern Hemisphere for the temperate biomes in North America and Europe, as well as the Tropical and Subtropical biomes in Africa. Our analysis provides quantitative insight as to how fire danger potential and fire behavior potential have been responding to changes in seasonal mean temperature and seasonal precipitation totals across different ecoregions around the world.

1. Introduction

Wildfires inherently occur in the Earth system, influencing land-atmosphere processes in biomes worldwide. Wildfires can impact ecosystem services by modifying the spatial distribution of fuels and redistribute carbon, water, and energy exchange between ecosystems and the atmosphere (Liu et al., 2019). These impacts highlight the concern about changes in fire activity, that is, the frequency and size of fires as quantified by fire occurrence and area burned, respectively (Flannigan et al., 2009; Westerling, 2016; Jain et al., 2022; Balch et al., 2022). Therefore, it is important to gain a quantitative understanding of the drivers influencing changes in fire activity for improving modeling and prediction studies and guiding adaptation strategies.

Many studies, such as Giglio et al. (2013); Andela et al. (2017); Schoennagel et al. (2017); Liu et al. (2019), commonly use wildfire statistics of fire occurrence and burned area to quantify fire activity. For example, Gillett et al. (2004) suggest that over the past four decades, Canada has been experiencing an increase in burned area due to anthropogenic warming. In the western region of the United States (US), studies indicate a higher frequency of large wildfires, longer wildfire durations, and longer wildfire season since the mid 1980s (Westerling et al., 2006; Abatzoglou and Williams, 2016). Li and Banerjee (2021) show that over the past two decades in California, the frequency of large fires has been decreasing but the burned areas have been increasing, suggesting that a smaller number of fires are becoming larger and more destructive. At a global scale, Doerr and Santín (2016) highlight that global burned area has been decreasing when compared against century long-term records. Turco et al. (2016) and Andela et al. (2017) also show decreases in burned area over the last few decades in Europe and around the world, respectively. In a review of global wildland fire activity, Flannigan et al. (2009) report that many studies show that burned area and fire occurrence will only continue to increase with a lengthening of the fire season and projected warmer temperatures. Though the spatiotemporal changes in fire frequency and size in response to a changing climate have been investigated in many studies, their conclusions differ, depending on the region and the time period being analyzed. While some studies show an increase in wildfire activity, others show a decrease, depending on the spatial and temporal scale over which the analysis was performed.

There is an increased need in understanding the weather and climate drivers influencing fire activity worldwide (Westerling et al., 2006; Marlon et al., 2008; Urrutia-Jalabert et al., 2018) in view of projected changes in the frequency, intensity, and duration of climatic extremes, such as droughts. Moreover, changes in climate and land-use/land cover regimes will affect not only the number of wildfires and area burned, but also where, for how long, and how intensely fires burn (Hanes et al., 2019; Williams et al., 2019; Li and Banerjee, 2021). Therefore, understanding the reasons for the spatiotemporal variations in wildfire frequency and fire size go beyond monitoring fire occurrence and burned area and require additional investigation on fire weather conditions that influence fire behavior potential and fire danger potential.

Fire weather conditions are often used to assess fire danger potential and fire behavior potential. Fire weather is characterized by high

temperatures, low relative humidity, and strong winds (Bedia et al., 2015; Richardson et al., 2022). Increased frequency of fire weather days has been globally prevalent in the past 40-years, priming the landscape to burn more frequently, because fire weather controls the timing and inter-annual variability in burned area (Jones et al., 2022). Increase in fire weather will subsequently impact vegetation dynamics, biogeochemical cycles, and physical and chemical atmospheric processes. Fire behavior is the manner in which a fire reacts to the influence of the ambient weather, fuels, and topography (e.g., the fire intensity, ignition, rate of spread) (National Wildfire Coordinating Group (NWCG), 2002) and fire danger is the sum of all danger factors that affect fire inception, spread, resistance to control, and subsequent fire damage (National Wildfire Coordinating Group (NWCG), 2002). Unlike fire activity, which quantifies fire statistics of actual fires, fire danger potential and fire behavior potential provide a likelihood estimate of what could possibly occur, not what has occurred.

Fire metrics, for example, the Canadian Fire Weather Index (FWI), Initial Spread Index (ISI), the Fosberg Fire Weather Index (FWDI), Hot Dry Windy index (HDW), and the McArthur Forest Fire Danger Index (FFDI) have been used in studies to analyze fire danger potential and its link to fire activity at regional and global scales. Richardson et al. (2022) examined changes in wildfire potential and used the 95th percentile of daily FFDI values to determine days that were conducive for fire weather. They showed that burned area increases when fire weather days follow drought conditions, predominant in southern Australia and the western US. Hawkins et al. (2022) analyzed the nature of several wind-driven wildfire events in the Western US and found that anthropogenic climate change has increased the likelihood of fire weather extremes (as determined by the FWI, ISI, FWDI, and HDW) by 40 % in regions where autumn wind-driven fires have occurred. Bedia et al. (2015) determined that there is a significant relationship between FWI and burned area and that the tropical and moist temperate broadleaf biomes are most sensitive to fire weather. Jain et al. (2022) analyzed trends in global fire weather extremes using the FWI and ISI and found that extremes in FWI have been increasing significantly for more than a quarter of the global burnable land mass. These studies are all important as they use additional fire metrics to understand changes in fire danger potential and fire behavior potential.

However, although investigations into changes in fire danger potential using fire metrics have been carried out, limited work has been conducted on identifying what specific aspects of fire behavior potential are changing, such as fire intensity potential and ignition potential. Furthermore, when investigating correlations or relationships between fire danger potential and fire behavior potential, there is a need to use fire metrics from different systems, such as the Canadian Forest Fire Danger Rating System (CFFDRS) and the US National Fire Danger Rating System (NFDRS), in order to ensure independent datasets and increase robustness of the findings. These limitations are the motivation for the current study.

This study offers a comprehensive analysis of the historical spatiotemporal changes in fire danger potential and fire behavior potential across the world by combining five novel approaches that differ from previous studies. One, this global study offers not only insight on how fire danger potential has

been changing but also delves into investigating how particular aspects of fire behavior potential may have changed over the past 40-years. This is conducted by analyzing fire danger potential using the FWI from CFFDRS and analyzing fire behavior potential using the Ignition Component (IC) and Energy Release Component (ERC) from the NFDRS. **Two**, this study offers analysis at the seasonal scale and provides added value on what seasons have been more prone to changes in fire behavior potential and fire danger potential. **Three**, previous studies have conducted global analysis on fire danger potential at relatively coarse resolution 1.5° or have used older versions of datasets, such as ERA Interim. This study provides a global analysis at a relatively high spatial resolution (0.25°), using the ERA5 reanalysis data, which is the most current and updated global reanalysis. **Four**, at such a high spatial resolution, this study offers additional context as to how changes in fire behavior potential and fire danger potential are changing with respect to differences in landcover vegetation types over different biomes around the world. **Five**, a correlation analysis is also conducted by using independent datasets of meteorological precipitation and temperature variables to compare changes in seasonal mean temperatures and seasonal precipitation totals to changes in fire danger potential and fire behavior potential.

Therefore, this study presents a comprehensive approach at comparing seasonal spatiotemporal changes (1980–2019) in fire danger potential (as quantified by FWI) in order to determine what seasons exhibit the greatest rate of increase across different vegetation and climate regimes (biomes). This comparison is repeated for fire behavior potential (fire intensity and ignition as quantified by ERC and IC, respectively) and provides the basis for quantitative insight into what characteristics of fire behavior potential may be changing and their relation to changes in seasonal precipitation totals and seasonal mean air temperature across biomes. Identifying the spatiotemporal trends in fire danger potential and fire behavior potential across biomes is important for assessing changes in wildfire impacts on diverse ecosystems.

2. Data and methods

2.1. Indices

A number of indices (Table 1) are used to examine the 40-year (1980–2019) seasonal changes in fire danger potential and fire behavior

potential (intensity and ignition) across 13 biomes around the world (Fig. 1). The biomes presented here represent intercontinental convergent ecosystems of natural communities and species with boundaries established from the World Wildlife Fund's Terrestrial Ecosystems of the World (Olson et al., 2001; Ellis et al., 2022).

In this study, fire danger potential is conceptualized by the Fire Weather Index System that is solely weather driven (Vitolo et al., 2020). FWI first describes the effects of atmospheric temperature, humidity, precipitation, and wind on fuel moisture and then the consequential effects on fire behavior potential if a fire is ignited (Di Giuseppe et al., 2016; Van Wagner, 1977; Van Wagner and Pickett, 1985). Therefore, FWI only quantifies fire danger potential and not actual fires (Vitolo et al., 2020).

The FWI system is a component in the Canadian Forest Fire Danger Rating System. It integrates temperature, relative humidity, wind speed, and rainfall into generating fuel moisture codes (Fine Fuel Moisture Code; Duff Moisture Code; Drought Code), which are then combined to produce an Initial Spread Index and Buildup Index. Collectively, these indices are used to quantify the FWI, an index that provides an overall rating of fire line intensity and the potential for fires to occur. FWI is used to inform the public of potential fire danger conditions (Copernicus Emergency Management Service (CEMS), 2022). It uses a numerical rating system and is dimensionless. Values that are >50 are considered extreme in many countries worldwide (Table 1). Although developed in Canada, FWI is used around the world because it can be adapted to local conditions in other regions, such as northern regions of the US and parts of Southeast Asia (WSL, 2012; NRC, 2020). It has been used to investigate regional trends in fire season (Jain et al., 2017) and global-scale attribution of observed fire weather trends (Jain et al., 2022). The FWI system has been integrated by the Global Fire Weather Database (GFWED) that provides different global FWI datasets using meteorological reanalysis or forecasts (Field, 2020). In addition, Abatzoglou et al. (2018) highlighted a strong correlation between FWI and burned area across certain non-arid ecoregions of the globe and noticed large correlations within the boreal and evergreen temperate forests of western North America. Bowman et al. (2017) also showed that high FWI values are frequently associated with extreme fire activities recorded using Fire Radiative Power observations. Therefore, FWI has been shown as a proven metric for quantifying fire danger potential at the global scale (Di Giuseppe et al., 2016, 2020), thus making it an

Table 1

Summary of the fire danger and fire behavior indices used in determining spatiotemporal trends in fire danger potential (Fire Weather Index); fire behavior potentials (Energy Release Component and Ignition Component).

Index	Description	Units & interpretation	Source
Fire danger potential			
Fire Weather Index (FWI)	Provides a metric of fire danger potential and represents the overall rating of fire line intensity by combining the rate of fire spread with the amount of fuel being consumed. FWI is used for general public information about fire danger conditions.	Dimensionless Numerical rating Values >50 are considered extreme for many countries	ERA5 (0.25°) 1980–2019 DOI: 10.24381/cds.0e89c522
Fire behavior potential			
Energy Release Component (ERC)	Provides a metric of fire intensity potential. Available energy (British Thermal Unit) per unit area (square foot) within the flaming front at the head of a fire. Value represents the potential heat release per unit area in the flaming zone and can provide guidance to several important fire activities. ERC values increase as live fuels cure and dead fuels dry, providing an indication of drought conditions.	25 Btu ft. ² -1 Open-ended relative values	ERA5 (0.25°) 1980–2019 DOI: 10.24381/cds.0e89c522
Ignition Component (IC)	Provides a metric of ignition potential and represents the probability that a firebrand will require suppression action.	(%) Values from 0 to 100 % 100 % means that every firebrand will cause a fire if it comes in contact with fuels that are receptive (opposite true for 0 %)	ERA5 (0.25°) 1980–2019 DOI: 10.24381/cds.0e89c522
Atmospheric drivers			
Temperature	Air temperature at 2 m height above the Earth's surface	(°C)	In-situ and satellite observations DOI: 10.24381/cds.11dedf0c
Precipitation	Flux of precipitation (rain, snow, hail) measured as the height of the equivalent liquid water	(mm/month)	In-situ and satellite observations DOI: 10.24381/cds.11dedf0c

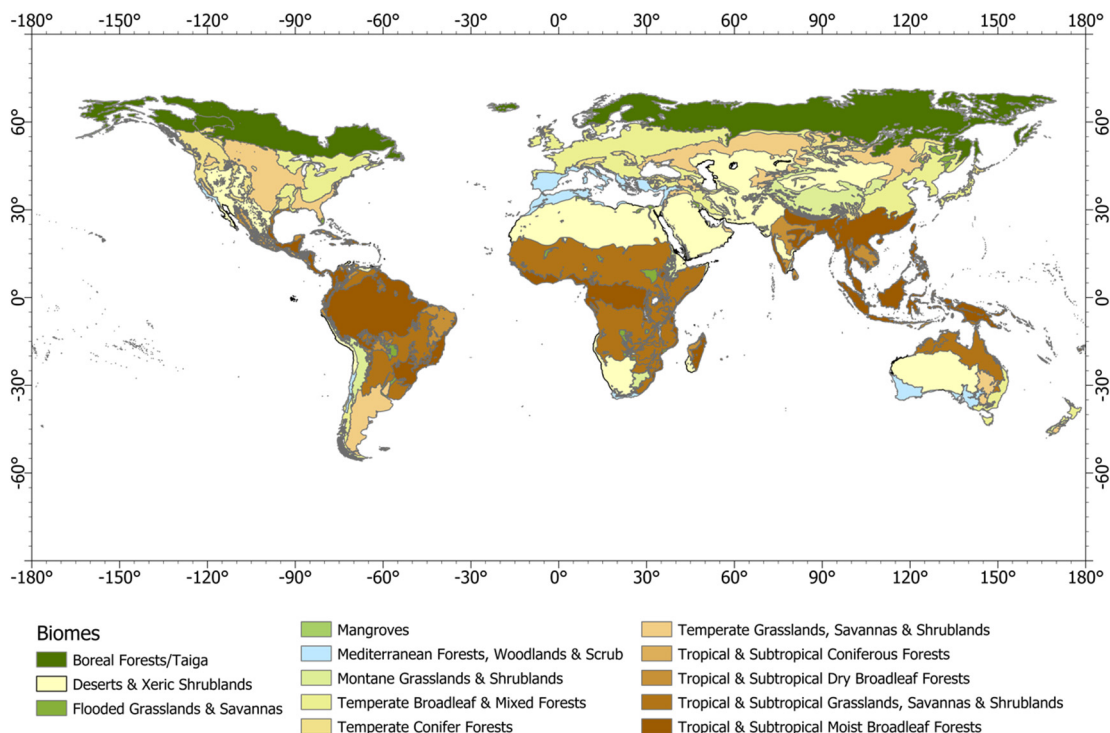


Fig. 1. Map of the 13 biomes analyzed across the world with overarching climates, including Tropical and Subtropical; Temperate and others

appropriate dataset for the current global study. The reader is referred to Van Wagner (1977, 1987) for more details on the computation of FWI.

In this study, the fire behavior indices represent conditions (fuel type, topography, and weather) that can influence specific characteristics of a fire, including fire intensity potential and ignition potential, as measured by the energy release component (ERC) and ignition component (IC), respectively (Di Giuseppe et al., 2016). ERC and IC are parts of a different system than FWI, the U.S. National Fire Danger Rating System (NFDRS) (Bradshaw et al., 1984). ERC is an indicator of the available energy of the flaming front at the head of a fire and represents the potential heat released per unit area in the flaming zone. Its unit is expressed in British Thermal Unit per square foot (BTU/ft²) with open-ended relative values (Copernicus Emergency Management Service (CEMS), 2022). ERC is driven from observations of maximum and minimum relative humidity, temperature, rainfall duration, cloudiness, slope class, fuel type and a fuel model that are subsequently used to calculate fuel moisture components of both dead fuels (1 h to 1000 h) and live fuels (National Wildfire Coordinating Group (NWCG), 2002). ERC values increase as live fuels are cured and dead fuels continue to dry. The NFDRS IC represents the probability that a firebrand will require suppression action. Expressed as a percentage, a high IC (such as 100 %) suggests that every potential firebrand will cause a fire that will require suppression attention if it comes in contact with receptive fuels. A value of 0 % indicates that no firebrand would cause a fire requiring suppression action when in contact with receptive fuels (Copernicus Emergency Management Service (CEMS), 2022). The numeric values of each NFDRS index are relative, for example, an IC value of 60 is interpreted as having twice the ignition probability of an IC of 30. By monitoring and establishing relationships between specific types of human caused fires and NFDRS indices, local managers are able to predict when to implement fire ban restrictions, such as limiting campfire activities.

The ERC and IC were selected for use in this study because they offer an independent proxy to understanding the influence of weather conditions on fire behavior that are separate from the behavior indices used in the CFFDRS FWI derivation (Initial Spread Index and Buildup Index). Although FWI has been more commonly used for global studies compared to ERC and IC, it is acknowledged that NFDRS indices can offer a first order approximation of the specific characteristics of fire behavior potential that could

be influenced by environmental conditions, offering additional insight as to why overall fire danger conditions are changing across the globe.

The fire indices are part of a large dataset provided by the Copernicus Emergency Management Service for the European Forest Fire Information System (EFFIS), a system that monitors and forecasts fire danger potential across Europe. EFFIS comprises a modeling component called the Global European Centre for Medium-Range Weather Forecasts (ECMWF) Fire Forecasting (GEFF) model. GEFF integrates NFDRS and the CFFDRS to provide a comprehensive set of outputs to characterize fire conditions at the global scale (Di Giuseppe et al., 2016, 2020; Vitolo et al., 2020). GEFF can produce fire danger potential and fire behavior potential indices in both reanalysis and forecast modes. The reanalysis data is part of an open data catalogue of the Copernicus Climate Data Store (Vitolo et al., 2020), and is used in this study.

A validation study examined the capability of the indices generated by the GEFF system (i.e., IC and FWI) to flag regions of high and low fire danger potential against actual observation fire events. The indices were able to flag above normal conditions that developed into fire events, as well as below normal conditions that did not develop into fires. While FWI outperforms IC in some parts of the world, this may be due to the fact that FWI only relies on weather inputs, while IC is highly dependent on information about the fuel and vegetation state. The NFDRS IC system requires accurate knowledge of vegetation green-up and curing in its original implementation. However in GEFF this information is read from mean climatological database, thus highlighting some shortcomings of a global system that relies on local knowledge. Nevertheless, since the intention of the GEFF system is to provide information at the global scale, some compromises had to be made (i.e., the substitution of human judgement at the local scale with mean climatological conditions). In contrast to FWI, the IC is slightly more cautious in predicting the potential for fire events, providing a lower false-alarm rate (Di Giuseppe et al., 2016). For these reasons, we find these indices are appropriate for the global analysis study and consider them a good first order approximation for the current analysis.

The fire danger potential data used in this study were acquired from the historical simulation, ECMWF Reanalysis 5th Generation (ERA5) (Copernicus Emergency Management Service (CEMS), 2022). The historical indices were acquired at the monthly scale from 1979 to present and a

global spatial coverage at 0.25° by 0.25° resolution. Based on the Integrated Forecasting System (IFS), ERA5 provides a record of the global atmosphere, land surface, and ocean waves. It replaces its outdated predecessor, ERA-Interim, by having a considerable increase in vertical and horizontal resolution, benefitting from a 10-year model and data assimilation development and offering an enhanced number of output parameters, such as wind at 100 m height. ERA5's assimilation system uses 12-h windows (0900-2100 UTC and 2100-0900 UTC the next day, inclusive). The observations within these windows are used and stored, hourly. A short forecast is generated from the analysis field at 9 h into each window (1800 and 0600 UTC) and provides a first guess for the next assimilation. ERA5 includes an advanced data assimilation system that is used to analyze land surface prognostic variables with a two-way interaction between the atmosphere and land (Hersbach et al., 2020). Furthermore, the atmosphere generates ocean waves through surface stress, and ocean waves influence the atmospheric boundary layer through the dependence of ocean surface roughness. Thus, all of ERA5 components are coupled through surface-atmosphere interactions. ERA5 is a trusted product because reanalyses provide contiguous spatial coverage and strive to ensure integrity and coherence in representing Earth system cycles. Reanalyses data are also trusted in climate monitoring applications and are now widely and routinely used by the World Meteorological Organization annual assessment of the State of the Climate, as well as by the IPCC (Dee et al., 2011; Hersbach et al., 2020) and thus their use is justified in the current study on wildfire climatology assessment.

2.2. Statistical methods

To statistically assess the annual rate of change (increase or decrease) in seasonal fire indices at each land grid cell across the globe at the 95 % confidence level, the Mann-Kendall Z statistic test (Z_{MK}) (Mann, 1945; Kendall, 1975; Gilbert, 1987; Kendall and Gibbons, 1990) and the Theil-Sen slope estimator (b_{sen}) (Theil, 1950; Sen, 1968) are employed. The Mann-Kendall test determines if there is a monotonic positive or negative trend based on the signum function (S) statistic for $(1 \leq i \leq j \leq n)$, where i and j are the i th and j th values in the time series (x) with length (n) (PNNL, 2022; Ellis et al., 2022).

$$S = \sum_{i=1}^{n-1} \sum_{j=i+1}^n \text{sgn}(x_j - x_i) \tag{1}$$

The S statistic is then normalized by the variance of the (S) statistic (VAR_S) to compute (Z_{MK}):

$$Z_{MK} = \begin{cases} \frac{S-1}{\sqrt{VAR_S}}, & S > 0 \\ 0, & S = 0 \\ \frac{S+1}{\sqrt{VAR_S}}, & S < 0 \end{cases} \tag{2}$$

where a positive (negative) value of (Z_{MK}) indicates whether the trend is increasing (decreasing) overtime.

The magnitude of the trend is then determined by (b_{sen}):

$$b_{sen} = \text{median} \left(\frac{x_j - x_i}{j - i} \right) \tag{3}$$

The Mann-Kendall test is ideal for this analysis as it estimates the linear regression nonparametrically, and the residuals from the fitted linear regression are not required to be normally distributed. The Mann-Kendall test is also less sensitive to outliers, thereby, making it ideal for testing long-term fire metric trends and has been used in other climatological trend analysis studies (Baijnath-Rodino et al., 2018, 2022; Ellis et al., 2022; Jain et al., 2022; Richardson et al., 2022).

Consider the seasonal time series of an index (i) for season (s) and for a particular land grid cell (l), $X_i(s, l) \in \mathbb{R}^m$, over the 1980–2019 period, where

$m = 40$ year. The Kendall-Theil method was used to calculate the slope at each grid cell at the 95 % confidence level ($p = 0.05$), following the methods by Helsel and Hirsch (1992). The normalized rate of change (expressed as %/yr) is then estimated as:

$$r_i(s, l) = \frac{\beta_i(s, l)}{\bar{X}_i(s, l)} \times 100 \in \mathbb{R} \tag{4}$$

where the slope, $\beta_i(s, l) \in \mathbb{R}$, represents the annual rate of change and $\bar{X}_i(s, l) \in \mathbb{R}$ represents the seasonal mean of the index i over the m -year period. The spatially averaged seasonal rate of significant change (either increase or decrease) of index (i) for season (s) over biome (b) is computed by:

$$\bar{r}_{i+}(s) = \frac{1}{n_{b+}(s)} \times \sum_{l \in \Omega_{b+}} r_i(s, l) \times [\Theta(0.05 - p_i(s, l))] \in \mathbb{R} \tag{5a}$$

$$\bar{r}_{i-}(s) = \frac{1}{n_{b-}(s)} \times \sum_{l \in \Omega_{b-}} r_i(s, l) \times [\Theta(0.05 - p_i(s, l))] \in \mathbb{R} \tag{5b}$$

where $p_i(s, l) \in \mathbb{R}$ represents the p -value of the MK test; Θ is the Heaviside step function, for which $\Theta(x) = 1$ iff $x \geq 0$ and 0 otherwise; Ω_{b+} and Ω_{b-} indicate domains in biome b for which $r_i(s, l) > 0$ and $r_i(s, l) < 0$, respectively; $n_{b+}(s) = \sum_{l \in \Omega_{b+}} \Theta(0.05 - p_i(s, l)) \in \mathbb{Z}_{\geq 0}$ and $n_{b-}(s) = \sum_{l \in \Omega_{b-}} \Theta(0.05 - p_i(s, l)) \in \mathbb{Z}_{\geq 0}$

represent the number of cells that have significantly positive and negative change, respectively. Note that a biome can exhibit both increases and decreases in fire danger potential within its areal coverage. The percentage of the biome's area with significant increase, $A_{b+}(s) \in \mathbb{R}$ and decrease, $A_{b-}(s) \in \mathbb{R}$, for each biome is defined as:

$$A_{b+}(s) = \frac{n_{b+}(s)}{N_b} \times 100 \tag{6a}$$

$$A_{b-}(s) = \frac{n_{b-}(s)}{N_b} \times 100 \tag{6b}$$

where $N_b \in \mathbb{Z}_{+}$ is the total number of land grid cells over the biome b .

Finally, this study also determines how 40-year seasonal timeseries in FWI correlates to that of observed seasonal precipitation totals and mean seasonal temperatures for each pixel across the globe:

$$c_p^{i,s} = \frac{\Sigma(i_y - \bar{i})(a_y - \bar{a})}{\sqrt{\Sigma(i_y - \bar{i})^2 \Sigma(a_y - \bar{a})^2}} \tag{7}$$

where ($c_p^{i,s}$) represents the correlation coefficient between the fire index (i) variable and the atmospheric variable (a) for a particular season (s) and pixel (p). The notations i_y and \bar{i} represent the seasonal fire index value for a specific year and the 40-year seasonal average fire index value, respectively. This is similar for the atmospheric variable. This step is repeated for IC and ERC and provides additional insights on the spatial and temporal atmospheric conditions influencing fire danger potential and fire behavior potential across the globe.

Furthermore, the temperature and precipitation data are made available by the Climatic Research Unit gridded Time Series (CRU TS) and provide an independent data source from that of ERA5 for the correlation analysis. CRU TS provides interpolated gridded data from weather observation stations to produce monthly, global (0.5°) resolution climate variables. Cross validation studies show that the mean absolute error of temperature and precipitation around the world are mostly below 1 °C and 40 %, respectively (Harris et al., 2020). This dataset has been widely used by many in the field of weather and climate (Harris et al., 2020) and is thereby deemed appropriate for use in this analysis.

3. Results and discussion

3.1. Fire danger potential

A spatial average of the rate of increase (decrease) in the fire danger potential for each biome, and the area of the biome affected (expressed as a percent) are computed. Results indicate that trends in fire danger potential are not homogenized around the world, and while some seasons and regions experience a significant decrease in fire danger potential, these changes are occurring at relatively lower rates and over smaller areas compared to increased fire danger potential (Fig. 2a&b). For example, although the Boreal Forest Biome has experienced a significant decrease in fire danger potential (<1.4 %/yr in all seasons) for an area < 2.6 % of its biome (750,000 km²) a significant rate of increase (between 1 and 1.6 %/yr for all seasons) is observed for an area between 1 and 8 million km² (4–26 %), a difference of area in one order of magnitude (Table A1). Hanes et al. (2019) indicate that trends in area burned and the frequency of large fires have increased significantly over the Canadian forests since 1959 and this may be related to an increase in lightning-caused fires. All biomes exhibit a decrease in fire danger potential, but this is present in <5 % of any given biome, whereas areas exhibiting increases in fire danger potential can range between 5 and 70 % (Fig. 2a). Considering that the increase in fire danger potential is more globally prevalent, this discussion, thereby, focuses primarily on analyzing the increases in fire danger potential, fire behavior potential, and potential atmospheric drivers across the biome.

Compared to all seasons, the SON season exhibits the greatest rate of significant increase (an average of 1.5 %/yr across all biomes) in fire danger potential (Fig. 3), followed by JJA, DJF, and MAM (Table A2). However, the seasons exhibiting the greatest areas prone to significant rates of increase in fire danger potential are JJA, followed by SON, MAM, and DJF (Fig. A1). The length of the fire weather season has been increasing for many continents across the world between 1979 and 2013 (Jolly et al., 2015). August, for example, is known to be a peak fire activity month in many regions of the world, such as in North America, with a large number of fires (Williams et al., 2019). The length of the fire season has increased

by over two months since the 1980s (Westerling et al., 2006). The current analysis indicates that fire danger potential has in fact been increasing more substantially in the later part of the year (SON) in comparison to the other seasons.

Compared to all biomes during the SON season, the Flooded Grasslands & Savannas Biome exhibits the greatest percentage of its area experiencing a significant rate of increase in fire danger potential (69 %, 850,000 km²). However, it is the Tropical and Subtropical Moist Broadleaf Forests Biome that exhibits the largest area (>8.7 million km²) showing a significant rate of increase in fire danger compared to all other biomes. This significant rate of increase in fire danger potential is also predominant during the SON season (2.2 %/yr). Furthermore, it is the Southern Hemisphere that is mostly contributing to the increase in fire danger potential over the Tropical and Subtropical Moist Broadleaf Forests Biome during the SON season (Fig. 4 and Fig. A4). Global observations of burned area also show that this biome is most sensitive to fire weather changes (Bedia et al., 2015). Other Tropical and Subtropical biomes with varying vegetation types (dry broadleaf forests, coniferous forests, and grasslands savannas and shrubland) have been less prone to an increase (<1.6 %/yr) in fire danger potential over the past 40-years.

In contrast, the temperate biomes have been experiencing a relatively high rate of increase (>1.5 %/yr) in fire danger potential over all vegetation types (broadleaf and mixed forests; grasslands, savannas and shrublands; and conifer forests) in comparison to all other biomes. The temperate forests in Australia have also seen a significant historical (1987–2017) increase in the number of large wildfires (>10 km²) (Tran et al., 2020). Thus, this region is experiencing increasing fire weather conditions that are conducive to the development of more frequent wildfire events.

When considering the atmospheric drivers of fire danger potential, the results show that there is a strong positive and significant correlation between fire danger potential and mean air temperature for all seasons and many regions of the world. However, this is mostly predominant during JJA in the Northern hemisphere for the temperate biomes in North America and Europe, as well as the Tropical and Subtropical biomes in

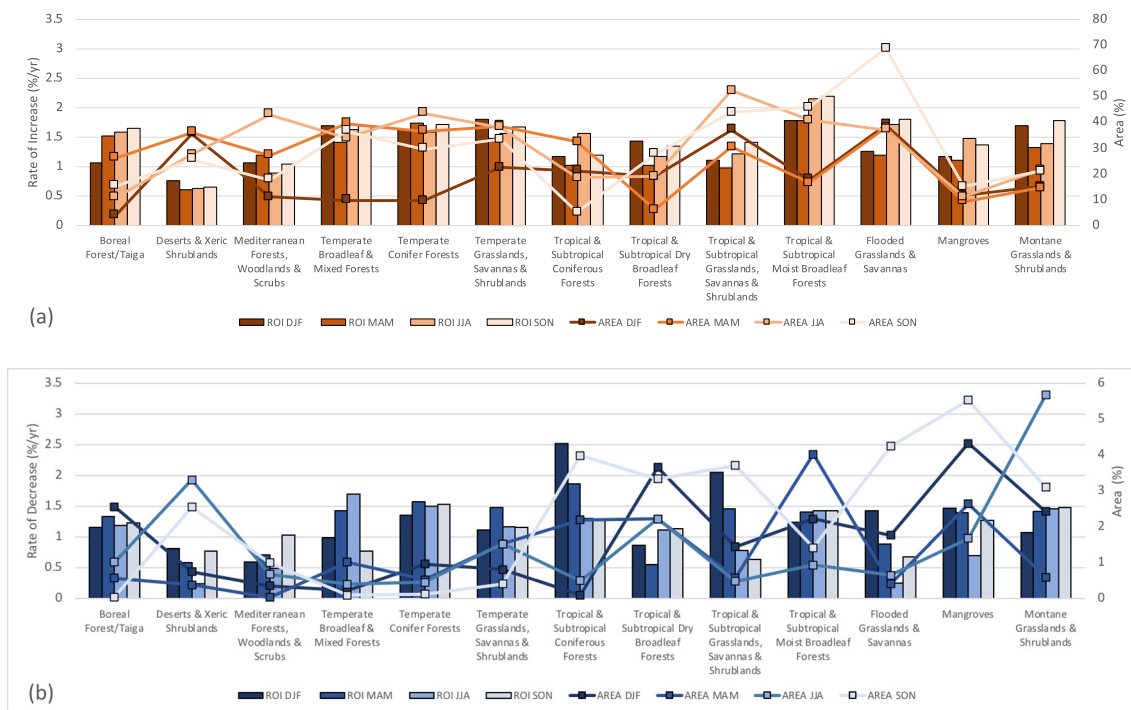


Fig. 2. Bar plots indicate the spatially averaged rate of significant change (%/yr) over the past four decades (1980–2019) in fire danger potential (as measured by FWI) over each biome for each season (DJF, MAM, JJA, SON), the line graphs represent the area of each biome (%) that exhibits a significant change in fire danger potential for each season; (a) shows the significant rate of increase (ROI) and corresponding area and (b) shows the significant rate of decrease and corresponding area for each season, note that the secondary axis representing area (%) in figures a and b have different ranges.

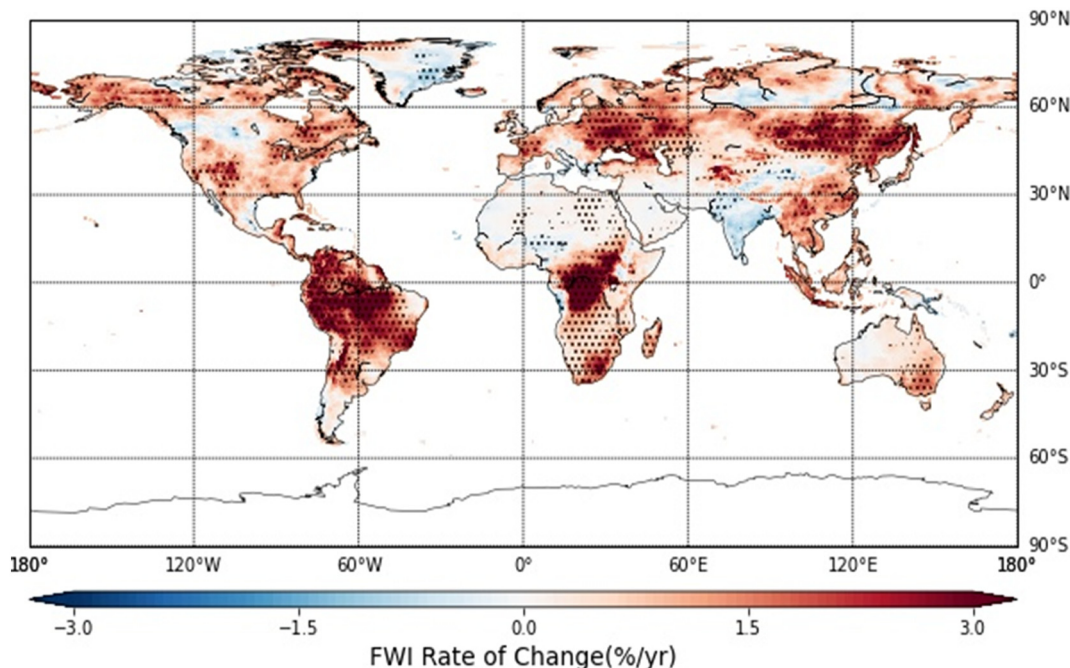


Fig. 3. The global distribution of the SON seasonal rate of increase (red) and decrease (blue) in fire danger potential over the past four decades (1980–2019) (%/yr) and the dotted regions representing significant trends at the 95 % confidence level. (For interpretation of the references to colour in this figure legend, the reader is referred to the web version of this article.)

Africa. In contrast, the Southern Hemisphere exhibits areas of stronger correlation during SON and DJF, with less correlation seen in Australia (Fig. 5a-d). However, the correlation between seasonal precipitation totals and fire danger potential are prevalent in Australia for all seasons. There is also a strong negative and significant correlation between JJA precipitation totals and fire danger potential in the temperate, boreal and Mediterranean biomes. This suggests that fire danger potential during the JJA season is strongly related to lower precipitation totals, within these biomes, irrespective of placement within the Northern or Southern Hemisphere (Fig. 6). Ellis et al. (2022) also shows that wildfire risk has increased across most ecoregions, highlighting a strong increasing trend in the number of days critical fuel moisture falls below a given threshold.

Similar studies, such as Jain et al. (2022) investigated historical trends in extreme annual FWI. They found a significant increase in FWI to be prevalent in over 26 % of the global burnable landscape, primarily driven by relative humidity, followed by temperature, precipitation, and then windspeed. Moreover, other studies that investigate fire activity show that approximately 80 % of global area burned occurs in grasslands and savannas that are primarily found in Africa, Australia, and South America

regions (Mouillot and Field, 2005). While fires occur globally, it is expected that grasslands and savanna regions will exhibit a greater change in fire danger potential and fire behavior potential than areas of sparse vegetation, such as the Sahara Desert in North Africa and the ice-covered landscapes of the Polar regions (Mouillot and Field, 2005; Flannigan et al., 2013). While all biomes are exhibiting an increase in fire danger potential, this study shows that the rate of increase in fire danger potential is substantially lower for the Deserts & Xeric Shrubland Biome, as well as the Mediterranean Forests, Woodlands & Scrubs Biome.

3.2. Fire behavior potential

The seasonal rate of increase in fire danger potential and the area affected in each biome are further contextualized through determining what characteristics of fire behavior potential are increasing during these seasons. The 40-year spatiotemporal rate of change in seasonal fire intensity potential, as measured by the energy release component is compared across biomes and seasons (Fig. A2). Results indicate that, on average over all biomes, fire intensity potential has been significantly increasing

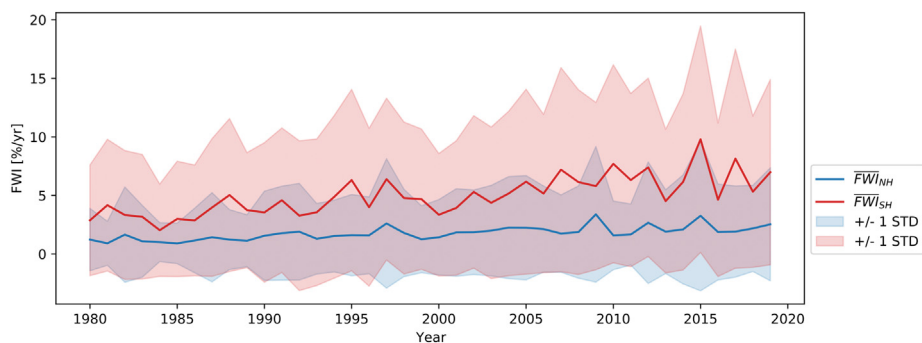


Fig. 4. The 1980–2019 timeseries of the average rate of increase in fire danger potential for the SON season for all pixels within the Tropical and Subtropical Moist Broadleaf Biome within the Northern Hemisphere (NH - blue) and the Southern Hemispheres (SH - red) that show a significant increase at the 95 % confidence level, where the blue shade and red shade represent the standard deviation in the Northern Hemisphere and Southern Hemisphere, respectively. (For interpretation of the references to colour in this figure legend, the reader is referred to the web version of this article.)

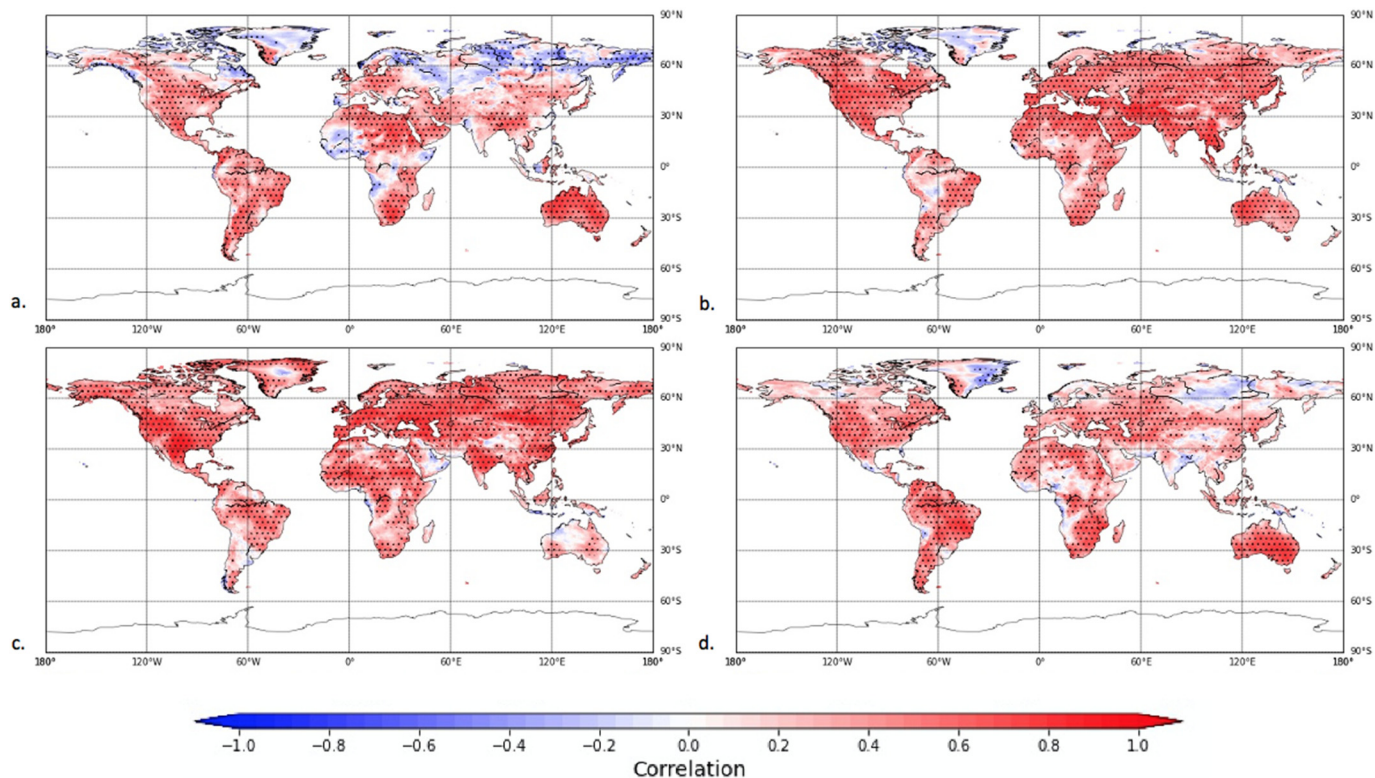


Fig. 5. Positive (red) and negative (blue) correlation between 40-year seasonal fire danger potential and seasonal mean temperature for (a) DJF, (b) MAM, (c) JJA, (d) SON, with black dots representing areas with significant correlation at the 95 % confidence level. (For interpretation of the references to colour in this figure legend, the reader is referred to the web version of this article.)

the most during the DJF season (>1.4 %/yr) (Fig. 7a&b, Table A2) and influenced mostly by the Northern Hemisphere. However, it is the MAM season that has been experiencing larger areas of increase within each biome (>12 %) (Fig. 8a), with both hemispheres contributing similarly to the increase (Fig. A5). In contrast, areas of significant decrease in fire intensity potential are <5 % in any given biome (similar to that of fire danger

potential) (Fig. 7a&b). Similar to the rate of increase in fire danger potential, fire intensity potential has also been increasing at a relatively higher rate for all vegetation types in temperate biomes (an annual average 1.8 %/yr) and this is predominant during the DJF season (Fig. 7 a&b). This is followed by a large rate of increase (1.7 %/yr) in the Tropical and Subtropical Moist Broadleaf Forests Biome for all seasons. However, for other

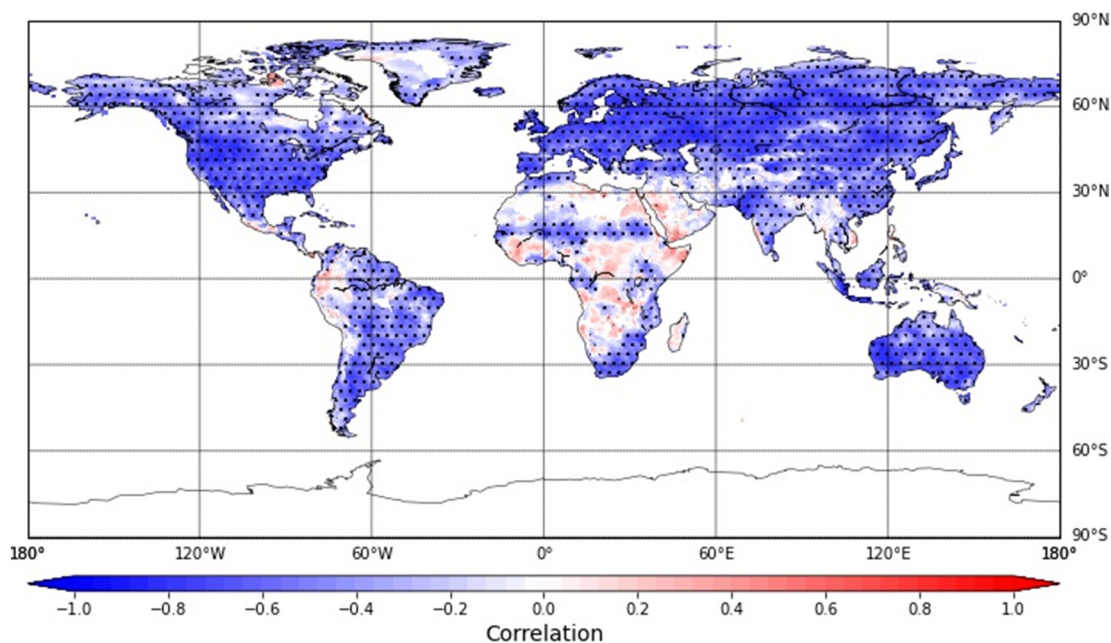


Fig. 6. Positive (red) and negative (blue) correlation between 40-year seasonal fire danger potential and seasonal precipitation totals for the JJA season. (For interpretation of the references to colour in this figure legend, the reader is referred to the web version of this article.)

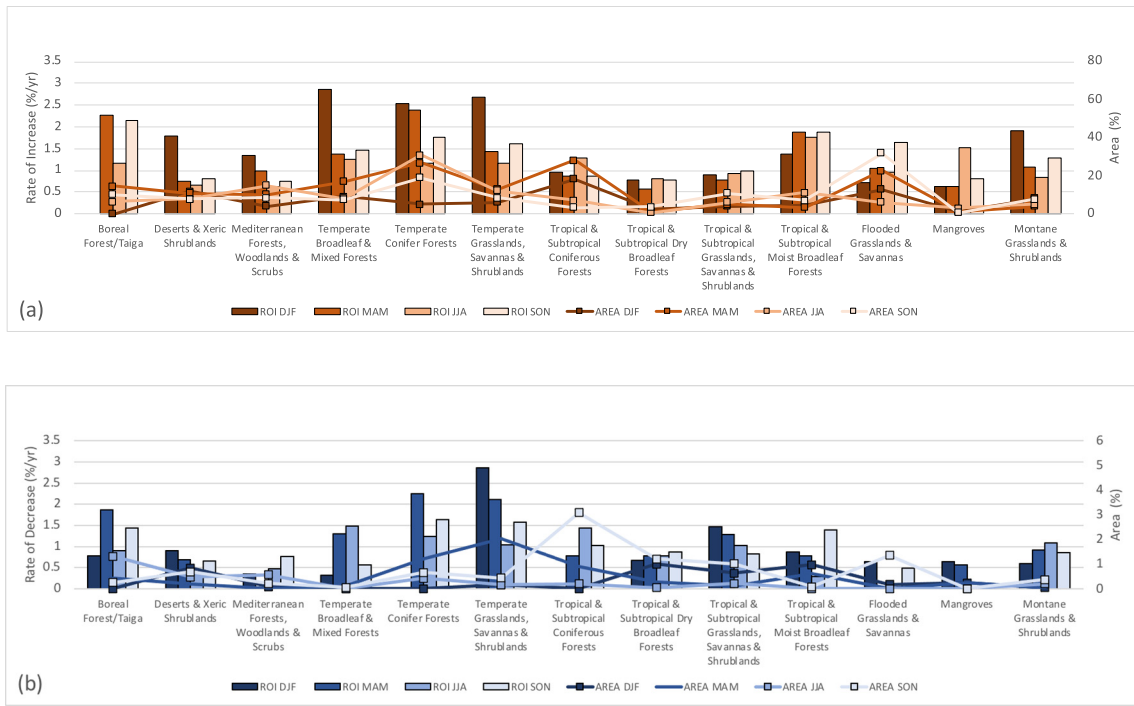


Fig. 7. Bar plots indicate the spatially averaged rate of significant change (%/yr) over the past four decades (1980–2019) in fire intensity potential (as measured by ERC) over each biome for each season (DJF, MAM, JJA, SON), the line graphs represent the area of each biome (%) that exhibits a significant change in fire intensity potential for each season; (a) shows the significant rate of increase and corresponding area and (b) shows the significant rate of decrease and corresponding area for each season, note that the secondary axis representing area (%) in figures a and b have different ranges.

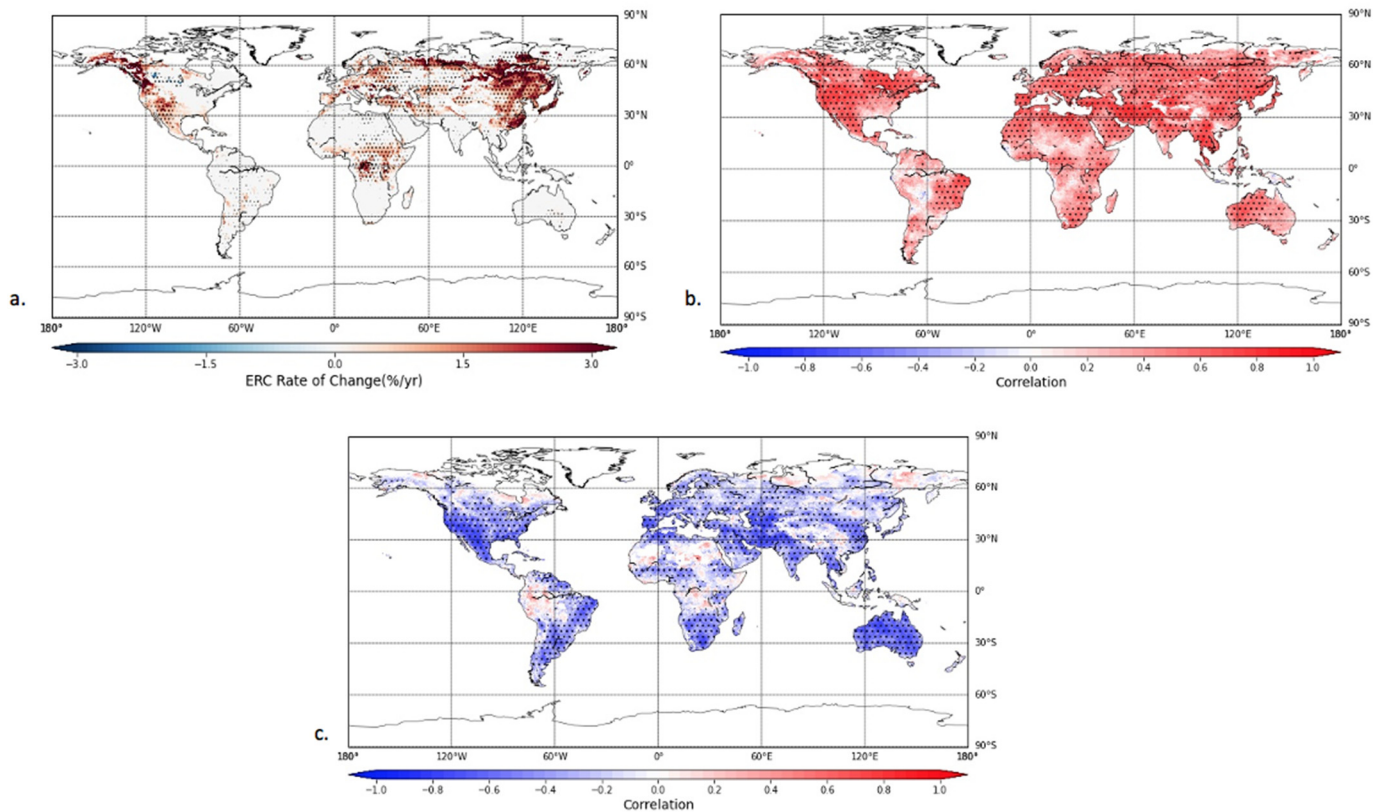


Fig. 8. (a) The global distribution of MAM season rate of increase (red) and decrease (blue) in fire intensity potential over the past four decades (1980–2019) (%/yr) with the dotted regions representing significant trends at the 95% confidence level. (b) Positive (red) and negative (blue) correlation between 40-year MAM fire intensity potential and seasonal mean temperature with black dots representing areas with significant correlation at the 95% confidence level, (c) same as (b), but correlation is between MAM fire intensity potential and seasonal precipitation totals. (For interpretation of the references to colour in this figure legend, the reader is referred to the web version of this article.)

vegetation types in the tropical and subtropical biomes, such as coniferous forests, grasslands, savannas, shrublands, and dry broadleaf forests, the rate of increase in fire intensity potential is relatively lower (<1.0 %/yr).

Compared to all other seasons, the increased air temperature and reduced precipitation totals during the MAM season tend to play a significant influence on the increase in fire intensity potential across most of the world. The MAM seasonal mean temperature exhibits strong, positive, significant correlations with fire intensity potential over a larger area of the world and is predominant in the Northern Hemisphere (Fig. 8b). This season also experiences strong negative and significant correlation between fire intensity potential and precipitation totals, that are predominant in North America's temperate biomes and western Asia's temperate biomes, as well as tropical biomes in eastern South America, and all biomes within Australia (Fig. 8c). Upward trends in global climate-related wildfire potential that is driven by increasing fire weather may likely be attributed to anthropogenic climate change from higher temperatures compared to rainfall (Richardson et al., 2022).

The rate of change in seasonal fire ignition potential, as measured by IC, represents the rate at which firebrands produce fires that will require suppression, resulting in spot fires. Compared to all months, the DJF and SON exhibit the greatest rate of increase in ignition potential when averaged over all biomes (1.4 %/yr), followed by MAM and JJA (Table A2). However, it is the MAM season that experiences the largest area (>1.6 million km² averaged over all biomes) in fire ignition potential increase, with both hemispheres contributing equally to the increases in fire ignition potential (Fig. A6). In addition, when averaged over all seasons, the temperate biomes (Temperate Conifer Forest Biome and the Temperate Broadleaf and Mixed Forest Biome) exhibit the greatest rate of increase in fire ignition potential (>1.8 %/yr over all seasons). In contrast, Deserts & Xeric Shrubland Biome, as well as the Mediterranean Forests, Woodlands & Scrubs Biome exhibit relatively less rate of increase in ignition potential compared to the other biomes. For example, averaged over all seasons, the Mediterranean Forests, Woodlands & Scrubs Biome shows an increase in fire ignition potential <0.9 %/year, for an area < 23 % of its biome (900,000 km²). The trends in fire ignition potential reflect similar spatiotemporal results to those of fire danger and fire intensity potential (Fig. 9a&b and Fig. A3).

3.3. Comparison between fire danger potential and fire behavior potential

The annual rates of increase in fire danger potential are compared against the fire behavior potentials (intensity and ignition) for each biome (Fig. 10). Overall, the temperate biomes exhibit the greatest rate of increase in fire danger potential and fire behavior potential combined (the Temperate Conifer Forest Biome, followed by the Temperate Grasslands, Savannas and Shrubland Biome and the Temperate Broadleaf and Mixed Forest Biome). In contrast, the Mangrove Biome experiences the least rate of increase in fire danger potential and fire behavior potential. The Mediterranean Forests, Woodlands and Scrubs Biome has the second lowest rate of increase in both fire behavior characteristics (intensity and ignition potentials) and fire danger potential. These results are in agreement with others who have reported a decrease in burned area in southern European countries between 1980–2011, including southern France, Greece, and Italy (Turco et al., 2016). In recent years, however, more European countries are experiencing large forest fires, such as in 2018, which can be attributed to record droughts and heat waves in the spring and summer of these years (Krikken et al., 2021). Seasonal droughts and heatwaves correspond to the time of year (June through September) when Europe is exhibiting increased fire danger potential, as seen in the current results and in agreement with Venäläinen et al. (2014). Recent attribution studies explain that global warming has slightly increased the risk of forest fires in Europe, in particular for Sweden, but the uncertainties are still considerable (Krikken et al., 2021).

Moreover, the Tropical and Subtropical Grasslands, Savannas and Shrublands Biome, which is very dominant in Africa, also exhibits one of the lowest rates of increase in fire behavior potential and fire danger. The Tropical and Subtropical Grasslands, Savannas, and Shrubland Biome has been experiencing significant rate of decrease in fire danger potential (>2.0 %/yr) in the DJF season over 300,000 km² (1.5 % of its area). This biome, which is predominant over Africa, exhibits a significant decrease in fire danger potential that is attributed to the decrease in vapor pressure deficit, an increase in rainfall, and an increase in net primary productivity (Zhao and Running, 2010; Hoscilo et al., 2014; Zubkova et al., 2019; Mamalakis et al., 2021). Africa tends to see an increase in air temperature

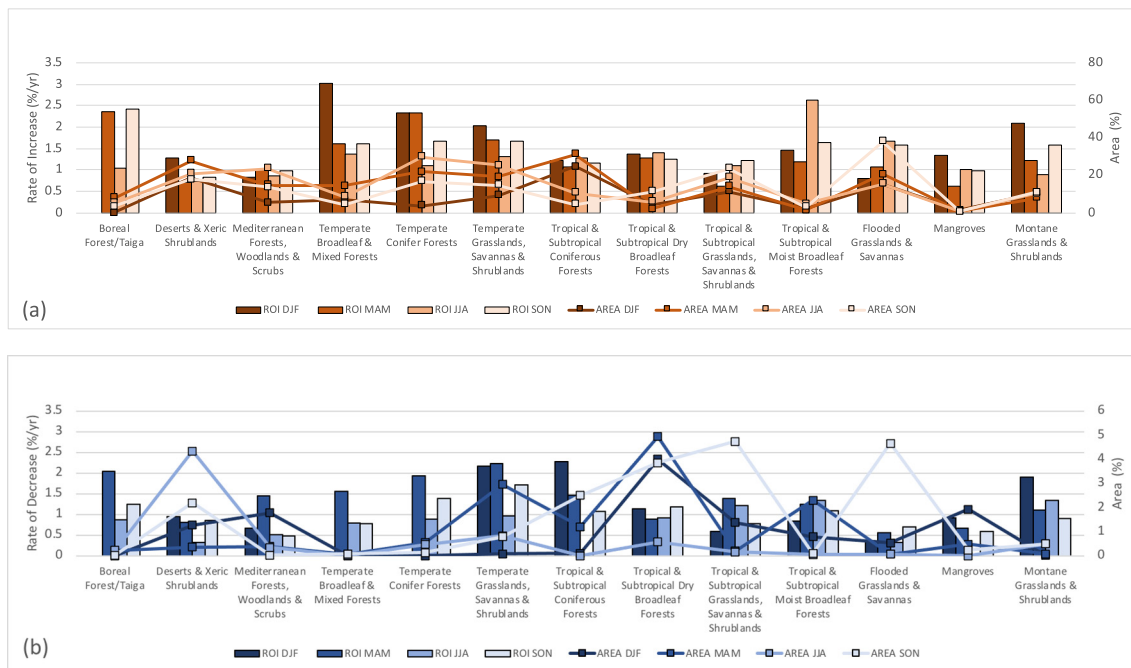


Fig. 9. Bar plots indicate the spatially averaged rate of significant change (%/yr) over the past four decades (1980–2019) in fire ignition potential (as measured by IC) over each biome for each season (DJF, MAM, JJA, SON), the line graphs represent the area of each biome (%) that exhibits a significant change in fire ignition potential for each season; (a) shows the significant rate of increase and corresponding area and (b) shows the significant rate of decrease and corresponding area for each season, note that the secondary axis representing area (%) in figures a and b have different ranges.



Fig. 10. Comparison of the relative proportion of the annual rate of increase (as denoted by the size of the block) in fire danger potential (FWI), fire intensity potential (ERC), and fire ignition potential (IC) for each biome over the past four decades (1980–2019).

from strong La Nina events, either causing the desiccation of fuels or additional precipitation that increases the availability of fuel for burning in subsequent years. Fires in Africa are attributed to the long dry season of the African savanna and the high rate of fuel accumulation, for which grass can regrow quickly after a fire (Archibald et al., 2009). However, fires in Africa are also driven by human activity, primarily during the years of 2002 to 2008 (Kouakou Kouassi et al., 2018; Kull and Laris, 2009). In addition, growing population has led to increased wildland fires being set for clearing fields, and converting savannas to agricultural lands in South Africa (Govender et al., 2006).

Increased fire danger and fire behavior can also have diverse impacts on ecosystems and the socio-economic structures for different regions of the world. For example, in North America, climate-driven insect outbreaks, such as by the mountain pine beetle can increase the frequency, extent, and severity of wildfires in North America because of their ability to reduce foliar moisture, alter chemistry, and increase flammability in fuels (Jolly et al., 2015; Coogan Sean et al., 2020). Climate change, influencing fire weather is also enhancing challenges in fire management and suppression in Canada as traditional approaches to fire suppression are reaching their economic and physical effectiveness limit (Podur and Wotton, 2010; Coogan Sean et al., 2020). The development in these wildland urban interface zones (WUI) has already exposed many communities to destructive fires, such as Fort McMurray fire, 2016 (Coogan Sean et al., 2020). The combination of anthropogenic warming, climate variability such as lightning, changes in management practices, all work in tandem and contribute to the increase in fire activity, changes in fire behavior, and drought conditions observed across North America.

In South America, land-use change is prevalent over forested regions. Starting in the 1970s, areas in south-central Chile experienced profound degradation to its native forests, being replaced by extensive matrix of exotic forest plantation mainly composed of *Pinus radiata* and Eucalyptus. This land-use change has altered the fuel structure, load, and flammability of the landscape, for which most fire activity in Chile is concentrated in this region of burnable biomass (Holz et al., 2012; Urrutia-Jalabert et al., 2018). Fires are also used for clearing land for agriculture, livestock, and other agrarian reform. Burning has been traditionally carried out without appropriate techniques or control to ensure positive outcomes, thus leading to fires spreading out of control, destroying vegetation, property and leading to additional adverse ecological conditions (González-Cabán, 2008). Fire danger metrics are closely related to fuel consumption and inversely correlated with vegetation productivity. Jolly et al. (2015) show that the length of the fire season (as determined by a metric) over the tropical and subtropical forests, grasslands and savannas and xeric shrublands of South America accounts for close to 30 % of the variation in global net land carbon flux.

Likewise, in Asia, human initiated fires are used for clear cutting in Eastern Ghats and northeast India, Chittagong hill tracts of Bangladesh, Myanmar, Sarawak in Malaysia, Philippines, Jambi, Sumatra and other parts in Indonesia, northern Thailand, northern Laos, Cambodia, and northern Vietnam. Fires are also used to clear residual agriculture to prepare the

land for the next crop season. For example, fires are usually used for clearing land for oil palm expansion in Indonesia. The years 2003 to 2016 also showed significant increase in fire activity over parts of Pakistan, India, Cambodia and Vietnam with increase in fire radiative power. The significant influence of land use and land cover changes in altering fire regime can be seen over these regions, especially in Sumatra and Kalimantan where peatlands have been drained for other use besides acting as natural forests. As a result, these regions are becoming flammable and progressively degrading, contributing to the increase in fire activity over the last two decades (Vetrita et al., 2021).

4. Conclusions

This study offers a comprehensive analysis of the historical spatiotemporal changes in seasonal fire danger potential and fire behavior potential for different biomes of the world over the 1980 to 2019 period. Results indicate that fire danger potential has been increasing significantly across all biomes, but at a higher rate in SON, followed by JJA, DJF, and MAM. The biome exhibiting the greatest rate of increase in fire danger potential is the Tropical and Subtropical moist broadleaf forests, which affects a larger percentage of its biome compared to other biomes. Fire danger potential can be seen increasing in northern regions of South America, parts of central Africa, and South Asia. Similarly, all the temperate biomes exhibit the greatest rate of increase in fire intensity potential, as well as a rate of increase in fire ignition potential; however, this is mostly predominant during the DJF season.

When considering the atmospheric drivers of fire danger potential, the results show that there is a strong positive and significant correlation between fire danger potential and mean air temperature. This is predominant mostly during JJA in the Northern Hemisphere for the temperate biomes in North America and Europe, as well as the Tropical and Subtropical biomes in Africa. Likewise, a strong negative and significant correlation between JJA precipitation totals and fire danger potential is prevalent in the temperate, boreal and Mediterranean biomes. Although it was expected that both seasonal temperature and precipitation totals would have strong correlation with the fire indices (because they are used as inputs in the derivation of the fire indices) this work provided additional insight as to what seasons and regions exhibit significant correlation between fire danger potential indices and atmospheric drivers.

While this study investigates trends in fire danger potential and fire behavior potential based on daytime weather inputs, additional global-scale studies may benefit from exploring trends at different times of the day. This is because, nighttime conditions, for example, which often allow for fire suppression due to lower vapor pressure deficit and air temperatures, are now experiencing an increased frequency in flammable nighttime hours (for which vapor pressure deficit exceeds a certain threshold) (Balch et al., 2022). This study provides reasons for the increase in fire danger potential in certain regions of the world. However, determining other physical drivers that are most prominent in influencing changes in fire

regimes is still a topic of great interest as increasing wildfire activity continues to have significant effects on ecosystems and biodiversity, air quality, human health, and the overall climate system.

CRediT authorship contribution statement

Janine A. Baijnath-Rodino: Conceptualization; Data curation; Formal analysis;

Investigation; Methodology; Project administration; Resources; Software; Validation;

Visualization; Roles/Writing – original draft; Writing – review & editing.

Phong Le: Formal analysis; Investigation; Methodology; Resources; Software; Validation; Visualization; Roles/Writing – original draft; Writing – review & editing

Efi Foufoula-Georgiou: Formal analysis; Investigation; Methodology; Project administration; Resources; Software; Validation; Visualization; Roles/Writing – original draft; Writing – review & editing.

Tirtha Banerjee: Formal analysis; Investigation; Methodology; Project administration; Resources; Software; Validation; Visualization; Roles/Writing – original draft; Writing – review & editing.

Author contribution

Baijnath-Rodino conceptualized and initiated this work, performed the analysis and generated the figures, and write-up. Le assisted with the methods and results, analysis, and edits. Banerjee and Foufoula-Georgiou assisted with the analysis, edits, writing, and funding of this work.

Data availability

Data will be made available on request.

Declaration of competing interest

The authors declare that they have no known competing financial interests or personal relationships that could have appeared to influence the work reported in this paper.

Acknowledgements

Baijnath-Rodino and Banerjee acknowledge the funding support from the University of California Office of the President (UCOP) grant LFR-20-653572 (UC Lab-Fees). Banerjee also acknowledges the National Science Foundation (NSF) grants NSF-AGS-PDM-2146520 (CAREER), NSF-OISE-2114740 (AccelNet) and NSF-CPS-2209695; the United States Department of Agriculture (USDA) grant 2021-67022-35908 (NIFA); and a cost reimbursable agreement with the USDA Forest Service 20-CR-11242306-072. Foufoula-Georgiou acknowledges the support by the National Science Foundation (grants DMS-1839336 and ECCS-1839441), NASA's Global Precipitation Measurement program (grant 80NSSC19K0684), and the Center for Ecosystem Climate Solutions (CECS), funded by California Strategic Growth Council's Climate Change Research Program.

Appendix A. Supplementary data

Supplementary data to this article can be found online at <https://doi.org/10.1016/j.scitotenv.2023.161954>.

References

Abatzoglou, J.T., Williams, A.P., 2016. Impact of anthropogenic climate change on wildfire across western US forests. *Proc. Natl. Acad. Sci. U. S. A.* 113, 11770–11775.

Abatzoglou, J.T., Williams, A.P., Boschetti, L., Zubkova, M., Kolden, C.A., 2018. Global patterns of interannual climate–fire relationships. *Glob. Chang. Biol.* 24, 5164–5175. <https://doi.org/10.1111/gcb.14405>.

Andela, N., et al., 2017. A human-driven decline in global burned area. *Science* 356, 1356–1362.

Archibald, S., Roy, D.P., van Wilgen, B.W., Scholes, R.J., 2009. What limits fire? An examination of drivers of burnt area in Southern Africa. *Glob. Chang. Biol.* 15 (3), 613–630. <https://doi.org/10.1111/j.1365-2486.2008.01754.x>.

Baijnath-Rodino, J.A., Duguay, C.R., LeDrew, E., 2018. Climatological trends of snowfall over the Laurentian Great Lakes Basin. *Int. J. Climatol.* <https://doi.org/10.1002/joc.5546>.

Baijnath-Rodino, J.A., et al., 2022. Historical seasonal changes in prescribed burn windows in California. *Sci. Total Environ.*, 836 <https://doi.org/10.1016/j.scitotenv.2022.155723>.

Balch, J.K., et al., 2022. Warming weakens the night-time barrier to global fire. *Nature* 602, 442–448. <https://doi.org/10.1038/s41586-021-04325-1>.

Bedia, J., Herrera, S., Gutierrez, J.M., Benali, A., Brands, S., Mota, B., Moreno, J.M., 2015. Global patterns in the sensitivity of burned area to fire-weather: implications for climate change. *Agric. For. Meteorol.* 214–215, 369–379.

Bowman, D., Williamson, G., Abatzoglou, J., et al., 2017. Human exposure and sensitivity to globally extreme wildfire events. *Nat. Ecol. Evol.* 1, 0058. <https://doi.org/10.1038/s41559-016-0058>.

Bradshaw, Larry S., Deeming, John E., Burgan, Robert E., Cohen, Jack D., 1984. The 1978 National Fire-Danger Rating System: Technical Documentation. General Technical Report INT-169. U.S. Department of Agriculture, Forest Service, Intermountain Forest and Range Experiment Station, Ogden, UT.

Coogan Sean, C.P., Xinli, Cai, Piyush, Jain, Flannigan Mike, D., 2020. Seasonality and trends in human- and lightning-caused wildfires \geq 2ha in Canada, 1959–2018. *Int. J. Wildland Fire* 29, 473–485. <https://doi.org/10.1017/WF19129>.

Copernicus Emergency Management Service (CEMS), 2022. . accessed May 2022 <https://cds.climate.copernicus.eu/cdsapp#!dataset/10.24381/cds.0e89c522?tab=overview>.

Dee, D.P., et al., 2011. The ERA-Interim reanalysis: configuration and performance of the data assimilation system. *Q. J. R. Meteorol. Soc.* 137, 553–597.

Di Giuseppe, F., Pappenberger, F., Wetterhall, F., Krzeminski, B., Camia, A., Libertá, G., San Miguel, J., 2016. The potential predictability of fire danger provided by numerical weather prediction. *J. Appl. Meteorol. Climatol.* 55 (11), 2469–2491. <https://doi.org/10.1175/JAMC-D-15-0297.1> available from:

Di Giuseppe, F., Vitolo, C., Krzeminski, B., Barnard, C., Maciel, P., San-Miguel, J., 2020. Fire weather index: the skill provided by the European Centre for medium-range weather forecasts ensemble prediction system. *Nat. Hazards Earth Syst. Sci.* 20, 2365–2378. <https://doi.org/10.5194/nhess-20-2365-2020>.

Doerr, S.H., Santín, C., 2016. Global trends in wildfire and its impacts: perceptions versus realities in a changing world. *Philos. Trans. R. Soc. B.* 371, 20150345. <https://doi.org/10.1098/rstb.2015.0345>.

Ellis, T.M., Bowman, D.M.J.S., Jain, P., Flannigan, M.D., Williamson, G.J., 2022. Global increase in wildfire risk due to climate-driven declines in fuel moisture. *Glob. Chang. Biol.* 28, 1544–1559. <https://doi.org/10.1111/gcb.16006>.

Field, R.D., 2020. Evaluation of global fire weather database reanalysis and short-term forecast products. *Nat. Hazards Earth Syst. Sci.* 20, 1123–1147. <https://doi.org/10.5194/nhess-20-1123>.

Flannigan, M.D., Krawchuk, M.A., de Groot, W.J., Wotton, B.M., Gowman, L.M., 2009. Global wildland fire and climate change. *Int. J. Wildland Fire* 18, 483–507.

Flannigan, M.D., Cantin, A.S., de Groot, W.J., Wotton, M., Newbery, A., Gowman, L.M., 2013. Global Wildland Fire Season Severity in the 21st Century. <https://doi.org/10.1016/j.foreco.2012.10.022>.

Giglio, L., Randerson, J.T., van der Werf, G.R., 2013. Analysis of daily, monthly, and annual burned area using the fourth-generation global fire emissions database (GFED4). *J. Geophys. Res.-Biogeosci.* 118, 317–328.

Gilbert, R.O., 1987. Statistical Methods for Environmental Pollution Monitoring. John Wiley & Sons Inc., New York, NY 978-0-471-28878-7.

Gillett, N.P., Weaver, A.J., Zwiers, F.W., Flannigan, M.D., 2004. Detecting the effect of climate change on Canadian forest fires geophys. Res. Lett. 31, L18211.

González-Cabán, A., 2008. Proceedings of the Second International Symposium on Fire Economics, Planning, and Policy: A Global View. General Technical Report (GTR). 208. Pacific Southwest Research Station, Forest Service, U.S. Department of Agriculture, Albany, CA. <https://doi.org/10.2737/PSW-GTR-208> 720 p.

Govender, N., Trollope, W.S.W., Van Wilgen, B.W., 2006. The effect of fire season, fire frequency, rainfall and management on fire intensity in savanna vegetation in South Africa. *J. Appl. Ecol.* 43, 748–758. <https://doi.org/10.1111/j.1365-2664.2006.01184.x>.

Hanes, C.C., Wang, X., Jain, P., Parisien, M-A., Little, J.M., and Flannigan, M.D. n.d. Fire-regime changes in Canada over the last half century. *Canadian Journal of Forest Research*. 49(3): 256-269. doi:10.1139/cjfr-2018-0293.

Harris, I., Osborn, T.J., Jones, P., et al., 2020. Version 4 of the CRU TS monthly high-resolution gridded multivariate climate dataset. *Sci. Data* 7, 109. <https://doi.org/10.1038/s41597-020-0453-3>.

Hawkins, L.R., Abatzoglou, J.T., Li, S., Rupp, D.E., 2022. Anthropogenic influence on recent severe autumn fire weather in the west coast of the United States. *Geophys. Res. Lett.* 49, e2021GL095496. <https://doi.org/10.1029/2021GL095496>.

Helsel, D.R., Hirsch, R.M., 1992. Statistical methods in water resources. (available on-line as a pdf file at: [http://water.usgs.gov/pubs/twri/twri4a3/](http://water.usgs.gov/pubs/twri/twri4a3/Studies%20in%20Environmental%20Science)) Studies in Environmental Science. 49. Elsevier, New York [Accessed, 2022] https://www.epa.gov/sites/default/files/2016-05/documents/tech_notes_6_dec2013_trend.pdf.

Hersbach, H., Bell, B., Berrisford, P., Hirahara, S., Horanyi, A., Munzo-Sabater, J., 2020. The ERA5 global reanalysis. *Q. J. R. Meteorol. Soc.* 146, 1999–2049.

Holz, A., Kitzberger, T., Paritsis, J., Veblen, T.T., 2012. Ecological and climatic controls of modern wildfire activity patterns across south-western South America. *Ecosphere* 3 (11), 103. <https://doi.org/10.1890/ES12-00234.1>.

Hoschilo, A., et al., 2014. A conceptual model for assessing rainfall and vegetation trends in sub-Saharan Africa from satellite data. *Int. J. Climatol.* 35 (12), 3582–3592. <https://doi.org/10.1002/joc.4231>.

- Jain, P., Wang, X., Flannigan, M.D., 2017. Trend analysis of fire season length and extreme fire weather in North America between 1979 and 2015. *Int. J. Wildland Fire* 26 (12), 1009–1020.
- Jain, P., et al., 2022. Observed increases in extreme fire weather driven by atmospheric humidity and temperature. *Nat. Clim. Chang.* 12, 63–70. <https://doi.org/10.1038/s41558-021-01224-1>.
- Jolly, W.M., et al., 2015. Climate-induced variations in global wildfire danger from 1979 to 2013. *Nat. Commun.* 6, 7537.
- Jones, M.W., et al., 2022. Global and regional trends and drivers of fire under climate change. *Rev. Geophys.* 60, e2020RG000726. <https://doi.org/10.1029/2020RG000726>.
- Kendall, M., Gibbons, J.D., 1990. *Rank Correlation Methods*. 5th ed. Oxford University Press, London, England.
- Kouakou Kouassi, J.-L., Wandan, N.E., Mbow, C., 2018. Assessing the impact of climate variability on wildfires in the N'Zi River watershed in central Cote d'Ivoire. *Fire* 1, 36. <https://doi.org/10.3390/fire1030036>.
- Krikken, F., Lehner, F., Haustein, K., Drobyshev, I., Jan van Oldenborgh, G., 2021. Attribution of the role of climate change in the forest fires in Sweden 2018. 2021. *Nat. Hazards Earth Syst. Sci.* 21, 2169–2179 [doi:10.5194/nhess-21-2169-2021](https://doi.org/10.5194/nhess-21-2169-2021).
- Kull, C.A., Laris, P., 2009. Fire ecology and fire politics in Mali and Madagascar. *Tropical Fire Ecology: Climate Change, Land Use and Ecosystem Dynamics*. Springer, Berlin/Heidelberg, Germany, pp. 171–226.
- Li, S., Banerjee, T., 2021. Spatial and temporal pattern of wildfires in California from 2000 to 2019. *Sci. Rep.* 11, 8779. <https://doi.org/10.1038/s41598-021-88131-9>.
- Liu, Z., Ballantyne, A.P., Cooper, L.A., 2019. Biophysical Feedback of Global Forest Fires on Surface Temperature. <https://doi.org/10.1038/s41467-018-08237-z>.
- Mamalakis, A., et al., 2021. Zonally contrasting shifts of the tropical rainbelt in response to climate change. *Nat. Clim. Chang.* 1 (11), 143–151. <https://doi.org/10.1038/s41558-020-00963-x>.
- Mann, H.B., 1945. Non-parametric tests against trend. *Econometrica* 13, 163–171.
- Marlon, J.R., et al., 2008. Climate and human influences on global biomass burning over the past two millennia. *Nat. Geosci.* 1, 697–702.
- Mouillot, F., Field, C.B., 2005. Fire history and the global carbon budget: a 1° x 1° fire history reconstruction for the 20th century. *Glob. Chang. Biol.* 11, 398–420.
- National Wildfire Coordinating Group (NWCG), 2002. *Gaining an Understanding of the National Fire Danger Rating System: PMS 932*. NFES 2665.
- Natural Resource Canada (NRC), . . . <https://cwfis.cfs.nrcan.gc.ca/background/summary/fdr>.
- Olson, D.M., et al., 2001. Terrestrial ecoregions of the world: a new map of life on Earth. *Bioscience* 51 (11), 933–938.
- Pacific Northwest National Laboratory (PNNL), . . . Accessed September 2022 https://vsp.pnnl.gov/help/vsample/design_trend_mann_kendall.htm.
- Podur, J., Wotton, B.M., 2010. Will climate change overwhelm fire management capacity? *Ecol. Model.* 221, 1301–1309. <https://doi.org/10.1016/J.ECOLMODEL.2010.01.013>.
- Richardson, D., et al., 2022. Global increase in wildfire potential from compound fire weather and drought. *npj Clim. Atmos. Sci.* 5, 23. <https://doi.org/10.1038/s41612-022-00248-4>.
- Schoennagel, T., et al., 2017. Adapt to more wildfire in western North American forests as climate changes. *Proc. Natl. Acad. Sci. U. S. A.* 114, 4582–4590.
- Sen, P.K., 1968. Estimates of the regression coefficient based on Kendall's tau. *J. Am. Stat. Assoc.* 63 (324), 1379–1389. <https://doi.org/10.1080/01621459.1968.10480934>.
- Theil, H., 1950. A rank-invariant method of linear and polynomial regression analysis, I, II, III. *Proceedings Van De Koninklijke Nederlandse Akademie Van Wetenschappen*. 53, pp. 386–392 521–525, 1397–1412.
- Tran, B.N., Tanase, M.A., Bennett, L.T., Aponte, C., 2020. High-severity wildfires in temperate Australian forests have increased in extent and aggregation in recent decades. *PLoS ONE* 15 (11), e0242484. <https://doi.org/10.1371/journal.pone.0242484>.
- Turco, M., et al., 2016. Decreasing fires in Mediterranean Europe. *PLoS ONE* 11 (3), e0150663. <https://doi.org/10.1371/journal.pone.0150663>.
- Urrutia-Jalabert, Rocio, Gonzalez, M.E., Gonzalez-Reyes, A., Lara, A., Garreaud, R., 2018. Climate variability and forest fires in central and south-central Chile. *Ecosphere* 9 (4), e02171. <https://doi.org/10.1002/ecs2.2171>.
- Van Wagner, C.E., 1977. *A Method of Computing Fine Fuel Moisture Content Throughout the Diurnal Cycle*. 596. Petawawa Forest Experiment Station, Chalk River, ON Information Report PS-X-69.
- Van Wagner, C.E., 1987. . 37 pp. Available online at Development and Structure of the Canadian Forest Fire Weather Index System. Canadian Forestry Service Tech. Rep., p. 35. <http://cfs.nrcan.gc.ca/pubwarehouse/pdfs/19927.pdf>.
- Van Wagner, C.E., Pickett, T.L., 1985. Equations and FORTRAN Program for the Canadian Forest Fire Weather Index System. Canadian Forestry Service, Petawawa National Forestry Institute, Chalk River, Ontario Forestry Technical Report 33. 18 p.
- Venäläinen, A., Korhonen, N., Hyvärinen, O., Koutsias, N., Xystrakis, F., Moreno, J.M., Urbista, I.R., 2014. Temporal variations and change in forest fire danger in Europe for 1960–2012. 2014. *Nat. Hazards Earth Syst. Sci.* 14, 1477–1490. <https://doi.org/10.5194/nhess-14-1477-2014>. www.nat-hazards-earth-syst-sci.net/14/1477/2014/.
- Vettrita, Y., Cochrane, M.A., Suwarsono, P.M., Sukowati, K.A.D., Khomarudin, M.R., 2021. Evaluating accuracy of four MODIS-derived burned area products for tropical peatland and non-peatland fires. *Environ. Res. Lett.* 16, 035015. <https://doi.org/10.1088/1748-9326/abd3d1>.
- Vitolo, C., et al., 2020. ERA5-based global meteorological wildfire danger maps. *Sci. Data* 7, 216. <https://doi.org/10.1038/s41597-020-0554-z>.
- Westerling, A.L., Hidalgo, H.G., Cayan, D.R., Swetnam, T.W., 2006. Warming and earlier spring increase western US forest wildfire activity. *Science* 313, 940–943.
- Westerling, A.L.R., 2016. Increasing western US forest wildfire activity: sensitivity to changes in the timing of spring. *Philos. Trans. R. Soc. B* 371, 20150178. <https://doi.org/10.1098/rstb.2015.0178>.
- Williams, A.P., Abatzoglou, J.T., Gershunov, A., Guzman-Morales, J., Bishop, D.A., Balch, J.K., Lettenmaier, D.P., 2019. Observed impacts of anthropogenic climate change on wildfire in California. *Earth's Future* 7, 892–910. <https://doi.org/10.1029/2019EF001210>.
- WSL, 2012. Fire weather indices. <http://wiki.fire.wsl.ch> [Accessed, April 2020].
- Zhao, M., Running, S., 2010. Drought-induced reduction in global terrestrial net primary production from 2000 through 2009. *Science* 329 (5994), 940–943. <https://doi.org/10.1126/science.1192666>.
- Zubkova, M., Boschetti, L., Abatzoglou, J.T., Giglio, L., 2019. Changes in fire activity in Africa from 2002 to 2016 and their potential drivers. *Geophys. Res. Lett.* 46, 7643–7653. <https://doi.org/10.1029/2019GL083469>.